

## Articles

# Hydrometal Complexes with More than One Planar and Quasi-Planar Tetracoordinate Carbon Atom: From Hydrogen-Surrounded Pieces to the Rudiment of Hydrogen-Sealed Nanotubes

Yan-Bo Wu,<sup>†</sup> Cai-Xia Yuan,<sup>†</sup> Fei Gao,<sup>†</sup> Hai-Gang Lü,<sup>†</sup> Jin-Chang Guo,<sup>†,‡</sup> Si-Dian Li,<sup>†,‡</sup> Yue-Kui Wang,<sup>†</sup> and Pin Yang<sup>\*,†</sup>

*Institute of Molecular Science, Key Laboratory of Chemical Biology and Molecular Engineering of the Education Ministry, Shanxi University, Taiyuan 030006, and Institute of Materials Sciences and Department of Chemistry, Xinzhou Teachers' University, Xinzhou 034000, Shanxi, People's Republic of China*

Received January 19, 2007

The feasibilities of one- and two-dimensional extensions of previously reported  $CM_4H_4$  ( $M = Ni$  and  $Cu$ ) units, which may result in species with more than one independent planar or quasi-planar tetracoordinated carbon (ptC or qptC) atom, have been studied with ab initio density functional theory calculations, and the results reveal that such extensions are possible. Significantly, some of the located hydrogen-surrounded piecelike genuine minima in general form  $C_nM_{2n+2}H_{2n+2}$  ( $n = 3, 4$ ;  $M = Ni, Pd, Pt$ ) may be the first examples of hydrometal complexes with three or four ptC and qptC atoms, while hydrogen-sealed minima in general forms  $C_{5n}M_{5n+5}H_{10}$  and  $C_{6n}M_{6n+6}H_{12}$  ( $n = 2$ ,  $M = Ni, Pd$ ) also may be novel examples of nanotubes with a large number of qptC atoms. These species with more than one ptC or qptC show both aesthetic appeal and predictable characteristics from a practical perspective. No new elements or groups are introduced into the system during the extensions. The results can provide some helpful ideas to synthetic chemists in their exploration activities to obtain such interesting neutral substance in macroquantity.

## Introduction

Since the first proposal of the concept of the planar tetracoordinate carbon (ptC) by Hoffmann, Alder, and Wilcox et al. in 1970,<sup>1</sup> a large number of molecules have been studied both experimentally and theoretically. Currently, the search for and characterization of species with ptC or quasi-ptC (qptC) have been stand-alone research goals as they have some peculiar bonding features and may have practical applications in both catalyst and material sciences.<sup>1,2</sup> Nevertheless, if one were to survey all the work in this field, it would be easy to find that these studies mainly focused on species with merely a single ptC; little attention was paid to those with more than one ptC. Species with multiple ptC atoms, especially those that could form one-, two-, or three-dimensional (1D, 2D, or 3D) crystals, possess superior advantages over species with only a single ptC in real applications; thus, they also have been studied. For example, a class of reported species with two or three ptC atoms were achieved by bridging the known complexes containing one

ptC with some groups, such as  $-CH-$ ,  $-S-$ ,  $-CO-$ , etc.,<sup>3</sup> or with metal ions.<sup>4</sup> In another kind of species with more than one ptC, the ptC usually served as a ligand for other ptC atoms, and all ptC atoms were included in an outer structure composed of  $\pi$ -accepting and  $\sigma$ -donating ligands.<sup>3b,5</sup> A typical example<sup>5m</sup> once proposed by our group contains a six-membered inner ptC

(3) (a) Wang, Z.-X.; Schleyer, P. v. R. *Science* **2001**, 292, 2465. (b) Minyaev, R. M.; Gribova, T. N.; Minkin, V. I.; Starikov, A. G.; Hoffmann, R. *J. Org. Chem.* **2005**, 70, 6693. (c) Li, S.-D.; Ren, G.-M.; Miao, C.-Q. *J. Phys. Chem. A* **2005**, 109, 259. (d) Li, S.-D.; Guo, J.-C.; Miao, C.-Q.; Ren, G.-M. *J. Phys. Chem. A* **2005**, 109, 4133.

(4) Pancharatna, P. D.; Méndez-Rojas, M. A.; Merino, G.; Vela, A.; Hoffmann, R. *J. Am. Chem. Soc.* **2004**, 126, 15309.

(5) (a) Priyakumar, U. D.; Sastry, G. N. *Tetrahedron Lett.* **2004**, 45, 1515. (b) Pulst, S.; Arndt, P.; Heller, B.; Baumann, W.; Kempe, R.; Rosenthal, U. *Angew. Chem.* **1996**, 108, 1175; *Angew. Chem., Int. Ed. Engl.* **1996**, 35, 1112. (c) Choukroun, R.; Cassoux, P. *Acc. Chem. Res.* **1999**, 32, 494. (d) Choukroun, R.; Donnadieu, B.; Zhao, J.-S.; Cassoux, P.; Lepetit, C.; Silvi, B. *Organometallics* **2000**, 19, 1901. (e) Choukroun, R.; Lorber, C. *Eur. J. Inorg. Chem.* **2005**, 4683. (f) Heeres, H. J.; Nijhoff, J.; Teuben, J. H.; Rogers, R. D. *Organometallics* **1993**, 12, 2609. (g) Evans, W. J.; Keyer, R. A.; Ziller, J. W. *Organometallics* **1993**, 12, 2618. (h) Rosenthal, U.; Ohff, A.; Tillack, A.; Baumann, W.; Górls, H. *J. Organomet. Chem.* **1994**, 468, C4. (i) Burlakov, V. V.; Arndt, P.; Baumann, W.; Spannenberg, A.; Rosenthal, U.; Parameswaran, P.; Jemmis, E. D. *Chem. Commun.* **2004**, 2074. (j) Rosenthal, U. *Angew. Chem.* **2004**, 116, 3972; *Angew. Chem., Int. Ed.* **2004**, 43, 3882. (k) Suzuki, N.; Watanabe, T.; Iwasaki, M.; Chihara, T. *Organometallics* **2005**, 24, 2065. (l) Yam, V. W.-W.; Fung, W. K.-M.; Cheung, K.-K. *Angew. Chem.* **1996**, 108, 1213; *Angew. Chem., Int. Ed. Engl.* **1996**, 35, 1100. (m) Wu, Y.-B.; Yuan, C.-X.; Yang, P. *J. Mol. Struct.: THEOCHEM* **2006**, 765, 35.

\* To whom correspondence should be addressed. E-mail: yangpin33@hotmail.com.

<sup>†</sup> Shanxi University.

<sup>‡</sup> Xinzhou Teachers' University.

(1) Hoffmann, R.; Alder, R. W.; Wilcox, C. F., Jr. *J. Am. Chem. Soc.* **1970**, 92, 4992.

(2) Keese, R. *Chem. Rev.* **2006**, 106, 4787.

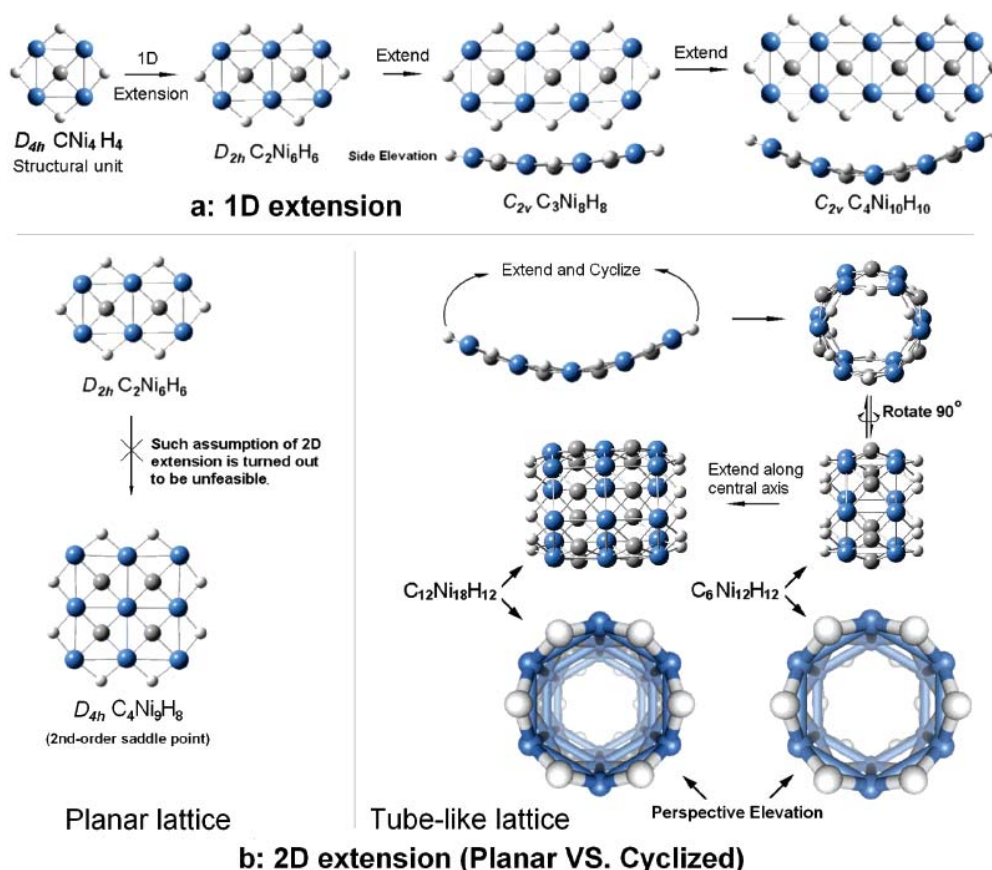


**Figure 1.** Road map of the one- and two-dimensional extension of the  $\text{CNi}_4\text{H}_4$  unit.

**Table 1.** Binding Energies of the Reactions  $n\text{C} + (2n + 2)\text{M} + (2n + 2)\text{H} \rightarrow \text{C}_n\text{M}_{2n+2}\text{H}_{2n+2}$  (BE, kcal/mol) and  $\text{M}_{2n+2}\text{H}_{2n+2} + n\text{C} \rightarrow \text{C}_n\text{M}_{2n+2}\text{H}_{2n+2}$  (RE, kcal/mol), Lowest Lying Vibrational Frequencies ( $V_{\min}$ ,  $\text{cm}^{-1}$ ), Energies of the HOMOs (eV), HOMO–LUMO Energy Gaps (eV), Total Wiberg Bond Indices of the Carbon Centers ( $\text{WBI}_{\text{C}}$ ) and Transition Metals ( $\text{WBI}_{\text{M}}$ ), Chemical Shifts of the Bridging Hydrogen Atoms ( $\delta_{\text{H}}$ ), and Calculated NICS(1) Values (ppm) of the Piecelike Complexes

	BE	RE	$V_{\min}$	HOMO energy	energy gap	$\text{WBI}_{\text{C}}$	$\text{WBI}_{\text{M}}$	$\delta_{\text{H}}$	NICS(1)
$D_{4h}$ $\text{CNi}_4\text{H}_4^a$	−533	−211	100	−5.77	2.98	3.65	1.71	4.6	−16.55
$D_{4h}$ $\text{CPd}_4\text{H}_4^a$	−590	−196	62	−6.71	3.52	3.57	1.56	2.5	−14.79
$D_{4h}$ $\text{CPT}_4\text{H}_4^a$	−619	−228	51	−6.88	3.44	3.77	1.86	2.2	−15.92
$D_{2h}$ $\text{C}_2\text{Ni}_6\text{H}_6$	−897	−413	27	−6.18	2.67	3.62	1.94/1.79	0.8	−13.01
$D_{2h}$ $\text{C}_2\text{Pd}_6\text{H}_6$	−961	−361	31	−6.71	2.92	3.53	1.83/1.67	−1.1/0.1	−10.56
$D_{2h}$ $\text{C}_2\text{Pt}_6\text{H}_6$	−1037	−376	34	−6.89	3.23	3.70	2.10/2.01	−1.4/0.2	−15.61
$\text{C}_{2v}$ $\text{C}_3\text{Ni}_8\text{H}_8$	−1252	−570	11	−6.18	2.27	3.59/3.60	2.02/1.81	−2.0/−0.3/−2.5	1 Å: −11.81/−6.13 −1 Å: −11.96/−5.91
$D_{2h}$ $\text{C}_3\text{Pd}_8\text{H}_8$	−1322	−513	14	−6.54	2.40	3.51/3.50	1.88/1.71	−1.4/−0.7/−1.8	−10.36/0.60
$D_{2h}$ $\text{C}_3\text{Pt}_8\text{H}_8$	−1444	−567	17	−6.59	2.59	3.69/3.66	2.17/2.10	−1.8/−1.4/−1.5	−14.32/−7.91
$\text{C}_{2v}$ $\text{C}_4\text{Ni}_{10}\text{H}_{10}$	−1607	−719	14	−6.26	2.19	3.60/3.56	2.06/2.02/1.80	−1.8/0.4/−1.8	1 Å: −14.57/−11.29 −1 Å: −8.89/−0.24
$D_{2h}$ $\text{C}_4\text{Pd}_{10}\text{H}_{10}$	−1680	−646	9	−6.52	2.17	3.49/3.49	1.92/1.91/1.72	−1.6/−0.9/−2.4	−10.10/−0.57
$D_{2h}$ $\text{C}_4\text{Pt}_{10}\text{H}_{10}$	−1846	−739	11	−6.47	2.27	3.67/3.65	2.22/2.21/2.12	−2.1/−1.9/−2.4	−13.69/−8.30

<sup>a</sup> These molecules are structural units for the extensions.

ring and a twelve-membered outer boron ring, so that the whole system looks like a beautiful wheel.

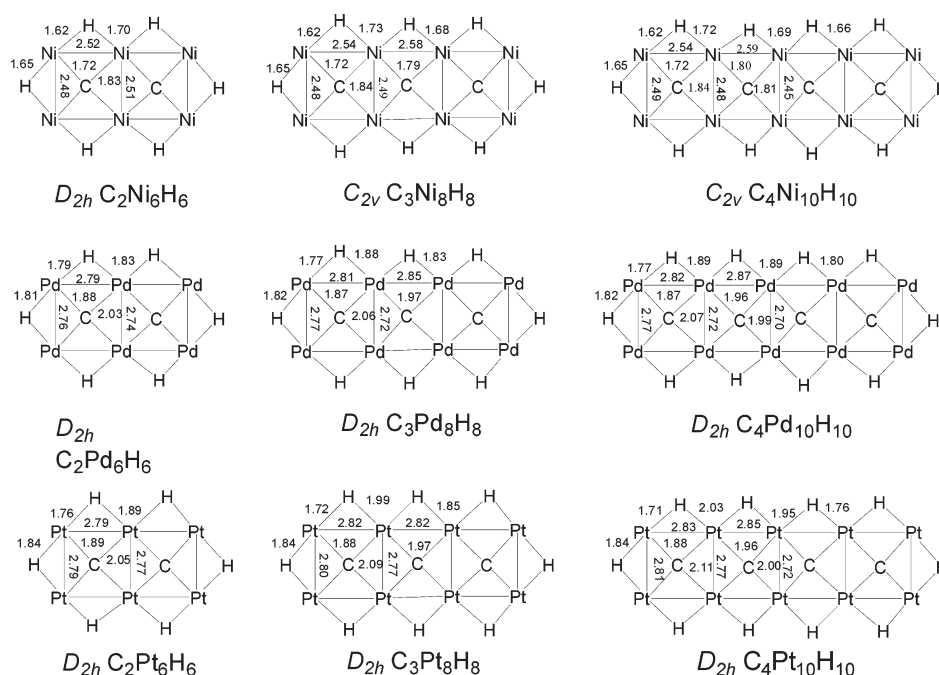
In the present work, the previously reported  $\text{CM}_4\text{H}_4$  ( $\text{M} = \text{Ni}, \text{Cu}$ ) species<sup>6</sup> were taken as the structural units to design species with multiple ptC atoms through natural extension in one or two dimensions. The road map of the extension of  $\text{CNi}_4\text{H}_4$  units is shown in Figure 1.

The results from the studies of 1D extensions revealed that when  $\text{M} = \text{Ni}$ , the extensions were viably possible, although we failed to obtain any energy minima for  $\text{M} = \text{Cu}$ . Thus the

counterparts of  $\text{M} = \text{Pd}$  and  $\text{Pt}$ , the heavier congeners of  $\text{Ni}$  were further investigated. On the basis of the 1D extension, we then investigated the 2D extension elementarily, and some genuine minima were located, revealing some species with interesting nanotube structures. These species have at least one of the following three advantages over other reported species with multiple ptC atoms: First, all ptC atoms in the species obtained by 1D and 2D extensions were not coordinated by other ptC atoms, which was propitious for the exertion of the characteristics of independent ptC atoms. Second, the regularly arranged ptC- or qptC- containing pieces and nanotubes can be taken as a beginning to form the 1D or 2D crystals. Last, no

(6) Li, S.-D.; Ren, G.-M.; Miao, C.-Q.; Jin, Z.-H. *Angew. Chem.* **2004**, *116*, 1395; *Angew. Chem., Int. Ed.* **2004**, *43*, 1371.

Chart 1 Structures of Piecelike Molecules with the Necessary Bond Lengths



new elements or bridging groups need to be introduced into such systems during the extension, which is advantageous for practical attempts to synthesize these neutral molecules in laboratories in the future, and we think that they may appear as the byproducts of  $CM_4H_4$  synthesis. However, the preparation of these complexes in laboratories is still a big challenge to experimental chemists.

### Computational Details

The geometric optimization and energy calculations were performed with the Gaussian03 program<sup>7</sup> based on the density functional theory (DFT) method. The Becke's three-parameter hybrid functional with the Lee–Yang–Parr correlation functional (B3LYP)<sup>8</sup> was employed for all calculations. For Ni-containing systems, two kinds of basis sets were used: i.e., 6-311++g\*\* was applied for all atoms, LANL2DZ was used for Ni atoms, and 6-311++g\*\* was applied for C and H atoms. Their essential results are not different, so the same mixed basis set was used for Pd- and Pt-containing systems. Once an optimized geometry was obtained, imaginary frequencies were checked at the same level by vibration analysis to verify the genuine minimum on the potential energy surface (PES) and to evaluate the zero-point energy (ZPE) correc-

(7) Frisch, M. J.; Trucks, G. W.; Schlegel, H. B.; Scuseria, G. E.; Robb, M. A.; Cheeseman, J. R.; Montgomery, J. A., Jr.; Vreven, T.; Kudin, K. N.; Burant, J. C.; Millam, J. M.; Iyengar, S. S.; Tomasi, J.; Barone, V.; Mennucci, B.; Cossi, M.; Scalmani, G.; Rega, N.; Petersson, G. A.; Nakatsuji, H.; Hada, M.; Ehara, M.; Toyota, K.; Fukuda, R.; Hasegawa, J.; Ishida, M.; Nakajima, T.; Honda, Y.; Kitao, O.; Nakai, H.; Klene, M.; Li, X.; Knox, J. E.; Hratchian, H. P.; Cross, J. B.; Adamo, C.; Jaramillo, J.; Gomperts, R.; Stratmann, R. E.; Yazyev, O.; Austin, A. J.; Cammi, R.; Pomelli, C.; Ochterski, J. W.; Ayala, P. Y.; Morokuma, K.; Voth, G. A.; Salvador, P.; Dannenberg, J. J.; Zakrzewski, V. G.; Dapprich, S.; Daniels, A. D.; Strain, M. C.; Farkas, O.; Malick, D. K.; Rabuck, A. D.; Raghavachari, K.; Foresman, J. B.; Ortiz, J. V.; Cui, Q.; Baboul, A. G.; Clifford, S.; Cioslowski, J.; Stefanov, B. B.; Liu, G.; Liashenko, A.; Piskorz, P.; Komaromi, I.; Martin, R. L.; Fox, D. J.; Keith, T.; Al-Laham, M. A.; Peng, C. Y.; Nanayakkara, A.; Challacombe, M.; Gill, P. M. W.; Johnson, B.; Chen, W.; Wong, M. W.; Gonzalez, C.; Pople, J. A. *Gaussian 03*, revision A.1; Gaussian, Inc.: Pittsburgh, PA, 2003.

(8) (a) Becke, A. D. *J. Chem. Phys.* **1993**, *98*, 5648. (b) Lee, C.; Yang, W.; Parr, R. G. *Phys. Rev. B* **1988**, *37*, 785. (c) Vosko, S. H.; Wilk, L.; Nusair, M. *Can. J. Phys.* **1980**, *58*, 1200.

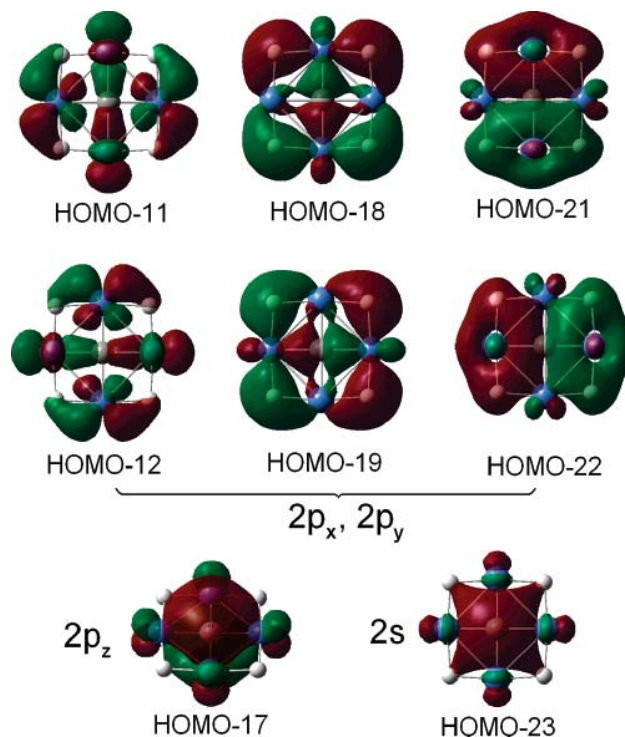


**Figure 2.** Pictures of the occupied MOs of the  $CNi_4H_4$  molecule involved in C–Ni bonding.

tion. The DFT wave functions obtained at optimized structures were

(9) (a) Schleyer, P. v. R.; Maerker, C.; Dransfeld, A.; Jiao, H.-J.; Hommes, N. J. R. E. *J. Am. Chem. Soc.* **1996**, *118*, 6317. (b) Wannere, C. S.; Corminboeuf, C.; Wang, Z.-X.; Wodrich, M. D.; King, R. B.; Schleyer, P. v. R. *J. Am. Chem. Soc.* **2005**, *127*, 5701. (c) Chen, Z.-F.; Wannere, C. S.; Corminboeuf, C.; Puchta, R.; Schleyer, P. v. R. *Chem. Rev.* **2005**, *105*, 3842.

(10) (a) Dodds, J. L.; McWeeny, R.; Sadlej, A. J. *Mol. Phys.* **1980**, *41*, 1419. (b) Wolinski, K.; Hilton, J. F.; Pulay, P. *J. Am. Chem. Soc.* **1990**, *112*, 8251.

(11) Carpenter, J. E.; Weinhold, F. *J. Mol. Struct.: THEOCHEM* **1988**, *169*, 41.



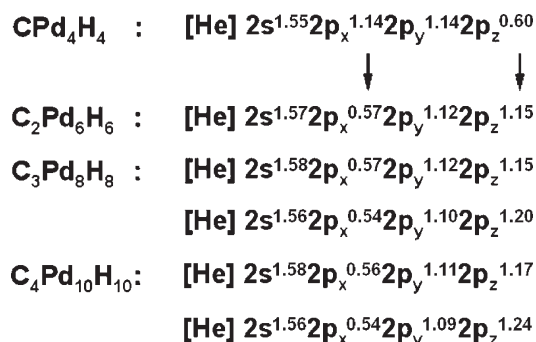


**Figure 3.** Electron configurations of the ptC atoms in the hydropalladium series of complexes.

confirmed to be stable. To assess the aromaticity of the 1D extended systems, the variation of relative NMR chemical shifts  $\delta_{\text{H}}$  of the bridging H atoms, and the nucleus-independent chemical shifts (NICSs)<sup>9</sup> for the ghost atoms located 1 Å above the centers of each  $M_4$  square were calculated with the gauge-independent atomic orbital (GIAO)<sup>10</sup> procedure. In addition, natural bond orbital (NBO)<sup>11</sup> analyses were carried out at the same theoretical level to explain the unique structures and bonding features of the complexes. In addition, to demonstrate the reasonability of our method and results starting from B3LYP/(LanL2DZ/ 6-311++G\*\*), another

basis set, with the same 6-311++G\*\* for C and H, and a pseudopotential basis set of CEP-31G or SDD for Pd and Pt were also applied and checked. Again, they give results similar to those from the LANL2DZ/6-311++G\*\* mixed basis set, with only one exception; namely, for the  $\text{C}_5\text{Pt}_{10}\text{H}_{10}$  molecule, B3LYP/(LANL2DZ/ 6-311++G\*\*) predicted a transition state (TS) with an imaginary frequency at 196i while the other two kinds of mixed basis sets predicted a genuine minimum on the corresponding PES. The detailed results starting from using the mixed sets of LANL2DZ/ 6-311++G\*\* for Ni-containing systems and those of CEP-31G/ 6-311++G\*\* and SDD/6-311++G\*\* for Pd- and Pt-containing systems can be found in the Supporting Information.

## Results and Discussion

**1. 1D Extensions. 1.1. Basis Characteristics.** The species located in 1D extensions have hydrogen-surrounded piecelike planar  $D_{2h}$  or quasi-planar  $C_{2v}$  structures (Chart 1). The carbon atoms in  $\text{C}_3\text{Ni}_8\text{H}_8$  and  $\text{C}_4\text{Ni}_{10}\text{H}_{10}$  ( $C_{2v}$ ) are pptC atoms, while those in the other molecules are all unambiguous ptC atoms. Table 1 gives the basic characteristics of these piecelike species and the structural units. The relatively larger binding energies (BEs) of the whole molecule demonstrate the stabilities of these complexes with respect to dissociation. It is noteworthy that the introduction of a carbon atom into each  $M_4$  square is

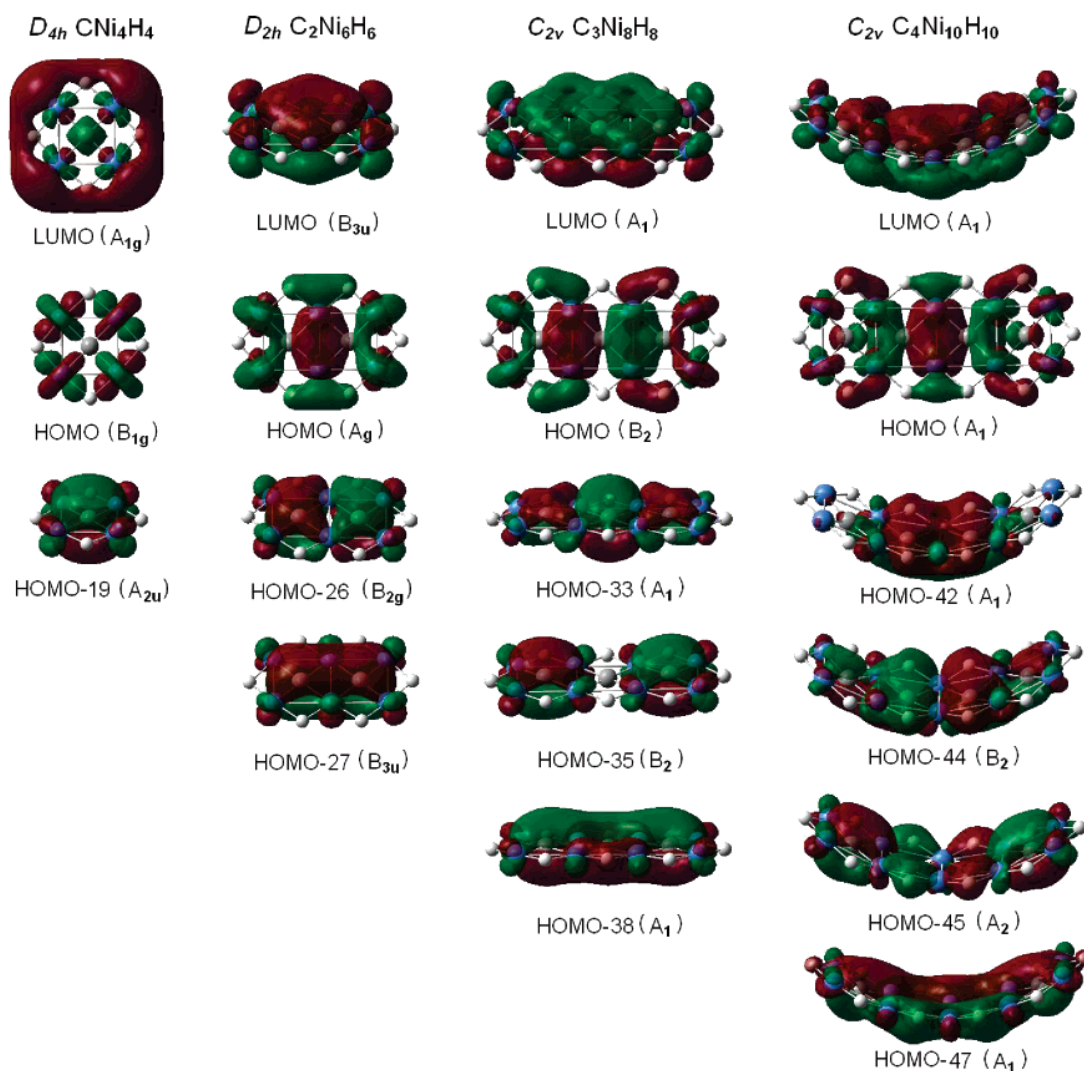


**Figure 4.** Plots of the LUMO, HOMO, and occupied  $\pi$  MOs (concerning the  $2p_z$  atomic orbitals of the carbon centers) of the hydronickel series.

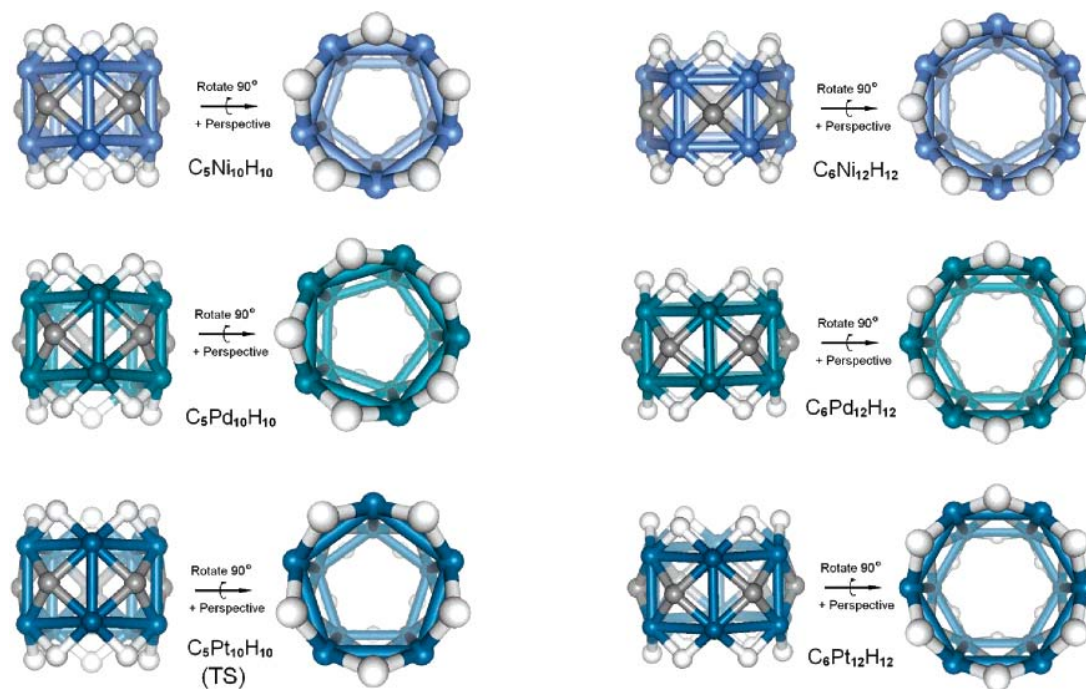


**Figure 5.** Structures of hydrogen-sealed barrel-like molecules.

essential for the stability, because the energies released (REs) from the reaction  $M_{2n+2}H_{2n+2} + nC \rightarrow C_nM_{2n+2}H_{2n+2}$  almost reach one-third of the BE, and without carbons in each  $M_4$  square, those  $M_{2n+2}H_{2n+2}$  frameworks would be TSs or high-order saddle points. As shown in Table 1, the energies of the highest occupied molecular orbital (HOMO) of these complexes are all lower than 6.20 eV, and the energy gaps between the HOMO and the lowest unoccupied molecular orbital (LUMO) are all more than 2.10 eV. This means that there does exist a stable singlet ground state.

If the present calculation results [with an increase of the number of carbons ( $n$ ) from 1 to 4, the corresponding C–M, M–M, and M–H bonds gradually stretch longer and the lowest lying vibrational frequencies ( $V_{\min}$ ; see Table 1) of the complexes also decrease to a degree] are analyzed isolatedly, we can come to the conclusion that the more the extension continues, the less stable the complexes become. However, the present calculations were performed in a vacuum, which is an ideal situation only; the stabilization effect of the solution and the formation of crystals have not been included. Although the calculations will become so large that they are beyond our computational resources as we take the aforesaid factors into account, still we are able to predict that the molecules will be stabilized under these effects. We even believe that the 1D extension should be continued limitlessly, at least to about 10 carbon atoms.

**1.2. Bonding Features.** When a structural unit is extended in one dimension as shown in Chart 1, the bonding geometry of the carbon atoms remains in planar tetracoordination while that of some M atoms will be changed from planar pentacoordination to planar or quasi-planar heptacoordination. The NBO analysis revealed that the total Wiberg bond indices (WBIs) for C atoms in ptC atom centers range from 3.49 to 3.77 while those for M ( $M = \text{Ni, Pd, Pt}$ ) atoms range from 1.56 to 2.22 (Table 1); both are much larger than the values of  $\text{WBI}_C = 2.32$  and  $\text{WBI}_{\text{Cu}} = 1.13$  in the  $\text{CCu}_4\text{H}_4$  molecule. Moreover, with an increase of  $n$  from 1 to 4 for  $M = \text{Ni, Pd, and Pt}$ , the corresponding values of  $\text{WBI}_C$  decrease while those of  $\text{WBI}_M$

increase gradually as shown in Table 1. We think that such variations facilitate the change in the bonding geometry of M atoms from planar pentacoordination to planar or quasi-planar heptacoordination. Therefore, we consider that the extendable characteristic of the  $\text{CM}_4\text{H}_4$  units is dominated partly by the bonding capacities of the M atoms.

**1.3. Aromaticity and Why the ptC Atoms in These Complexes Are Independent of Each Other.** The general strategy for the stabilization of molecules containing ptC centers would be to form an aromatic ring surrounding the above C center with ligands with  $\pi$ -accepting and  $\sigma$ -donating abilities.<sup>1,3b</sup> As the M atom can display both  $\sigma$ -donating character by giving its  $\sigma$  electron in the outer s orbital and  $\pi$ -accepting character by accepting electrons with its inner d orbitals, the above strategy should still be valid for the purpose of the present work. Our calculations revealed that it is the gradually enhanced aromaticity that takes responsibility as the driving force which leads to the retention of more than one ptC in a hydrometal complex. Such a conclusion can be understood as follows. First, the length of the C–M bond as shown in Chart 1 is similar to that of the organometallic C–M bond between the corresponding M atom and C atom on an aromatic ring such as benzene, which indicates that the C atoms are located in an aromatic environment. To obtain more information on C–M bonding, the detailed orbital analysis performed for the  $\text{CNi}_4\text{H}_4$  unit was taken as an example. The results revealed that there were eight orbitals involved in the C–Ni bonding (Figure 2), in which the first one was the combination of the 2s orbital of the C atom and the  $d_{z^2}$  orbitals of the surrounding Ni atoms, the second one was the combination of the  $2p_z$  orbital of the C atom and the  $d_{xz}$  or  $d_{yz}$  orbitals of the surrounding Ni atoms, and the others were the combination of the  $2p_x$  or  $2p_y$  orbital of the C atom and various d orbitals of the surrounding Ni atoms. All the data indicated that the carbon atom was in a binding status very similar to the  $sp^2$  hybrid state in an aromatic system. As the complement of orbital analysis, the electron density analysis



(using Molden package<sup>12</sup>) of the corresponding molecular orbitals is given in the Supporting Information, because the results agreed closely with the orbital analysis. Second, consistent with the above-mentioned result, the negative NICS values, as shown in Table 1, indicate that all  $M_4$  squares are aromatic in nature. Third, as shown in Table 1, the nuclear magnetic shielding tensors of the H atoms (31.9 ppm) in  $T_d$   $Si(CH_3)_4$  (TMS),  $\delta_H = -7.6$  ppm in benzene but  $\delta_H = 4.6$ , 2.5, and 2.2 ppm in  $CNi_4H_4$ ,  $CPd_4H_4$ , and  $CPt_4H_4$ , respectively, demonstrate that the location of the hydrogen atoms in these structural units has a ring-current effect of antiaromatic characteristic. However, when these units are extended, the  $\delta$  values of the bridging hydrogen atoms are gradually shifted upfield and most of them are negative, meaning that the aromaticity is enhanced with the extension.

NBO analyses can give us some answers to why the aromaticity is enhanced and why the ptC atoms in these complexes are independent of each other. Take the situation in the ptC-contained hydropalladium series of complexes as an example. Shown in Figure 3 are the electron configurations of the carbon atoms of these complexes. As the figure shows, when the  $CPd_4H_4$  unit is extended, the occupancy of the  $2p_x$  orbital of the ptC center decreases from 1.11 to less than 0.57 while that of the  $2p_z$  orbital increases from 0.60 to more than 1.15. It is obvious that the decrease in the occupancies of the  $2p_x$  orbitals decreases the possibility that the carbon atoms form a strong  $\sigma$  bond through the head-to-head mode (taken as the bonding axis), so all carbon atoms are relatively independent of each other, while the increase in the occupancy of the  $2p_z$  orbitals could stabilize the extended structures through the enhanced and highly delocalized  $\pi$  interactions. Shown in Figure 4 are the plots of the LUMO, HOMO, and occupied  $\pi$  orbitals (concerning the  $2p_z$  orbitals of the carbon centers) of the piecelike hydronickel series of complexes (those of the hydropalladium and hydroplatinum series of complexes are similar in shape; they are given in the Supporting Information). As the figure shows, the number of such  $\pi$  orbitals increases synchronously with the number of carbon atoms, indicating the aromaticity is gradually enhanced.

**2. 2D Extensions. 2.1. Two Projects of 2D Extensions.** The initial assumption of 2D extension of the structural units is shown on the bottom left side of Figure 1. Since we failed to locate any genuine minima in the corresponding PESs, we had to design a new method for 2D extensions. The results of the calculation for hydronickel, with which the global minima have the bent  $C_{2v}$  structures when the number of ptC atoms is equal to or larger than 3 in 1D extensions, enlighten us: the bending trend of the molecules makes it possible to cyclize the pieces. Although an ab initio study of cyclization reactions is beyond our computational resources, still the possibilities of the corresponding cyclic molecules could be examined. The calculations reveal that the three series of ptC- or qptC-containing hydronickel, hydropalladium, and hydroplatinum in 1D extension studies all have their corresponding cyclic molecules, and these are shown in Figure 5. They have the hydrogen-sealed barrel-like structure, in which all carbon atoms are qptC atoms. Although they are still the molecules of 1D extensions of the  $CM_4H_4$  units in nature, if the barrel-like structure could be extended along its central axis (see the bottom right side of Figure 1), such an extension could be regarded as the real 2D extension (from line to plane) of the structural units.

**2.2. Rudiments of Nanotubes.** We carried out calculations to explore the possibility of the existence of complexes derived from the second method mentioned above, and the results showed that such extensions are feasible for qptC-containing

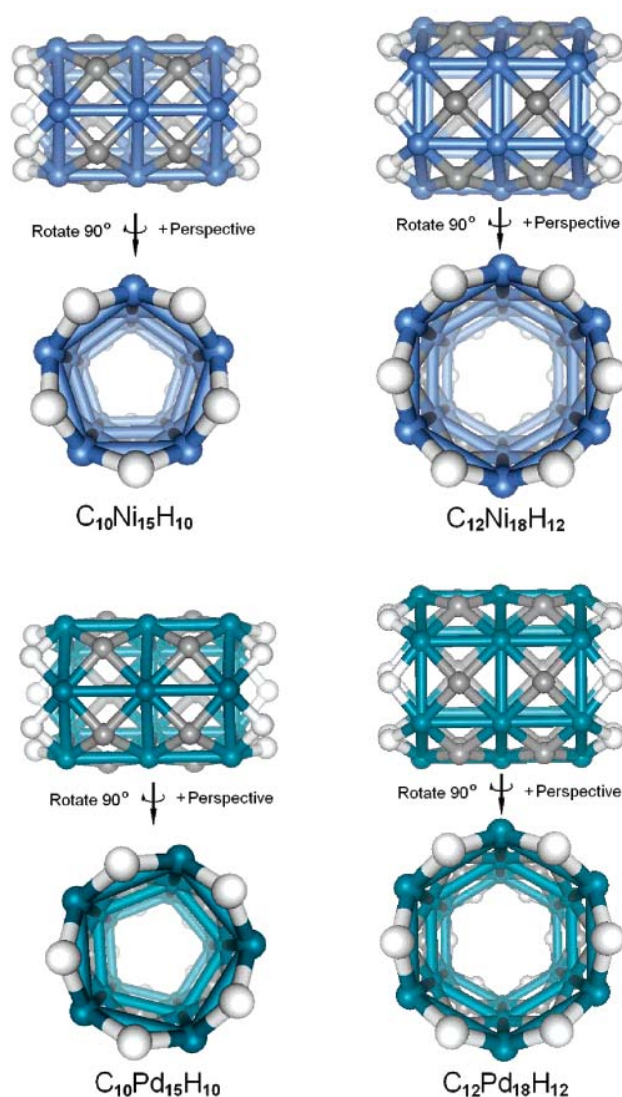


**Figure 6.** Structures of hydrogen-sealed tubelike molecules.

barrel-like hydronickel and hydropalladium molecules. The located genuine minima in the corresponding PESs are shown in Figure 6. In these species, the bonding geometries of the M atoms in the middle column have been converted from quasi-planar heptacoordination to quasi-planar octacoordination while the carbon atoms still keep the geometry of quasi-planar tetracoordination. As the quasi-planar octacoordination is possible for nickel and palladium, we can predict that it is also possible to further extend these tubelike structures along their central axes, which would bring amazing nanotube structures containing a large number of qptC atoms.

**2.3. Basic Characteristics and Bonding Features.** The basic characteristics of the species in cyclic form are summed up in Table 2. They all have barrel-like or tubelike structures sealed by bridging hydrogen atoms, and their general formulas are  $C_{5n}M_{5n+5}H_{10}$  and  $C_{6n}M_{6n+6}H_{12}$  ( $n = 1, 2$ ;  $M = Ni, Pd$ , and  $Pt$ ). As shown in Table 2, the basic characteristics and bonding features of these barrel-like molecules are similar to those of the above-mentioned piecelike species, as they belong to 1D extensions from the  $CM_4H_4$  unit. However, compared with those of barrel-like molecules, the lengths of the M–M bonds and M–C bonds concerning quasi-planar octacoordinate M atoms in the corresponding tubelike molecules have stretched; the values of  $WBI_M$  of the M atoms with quasi-planar heptacoordination and  $WBI_C$  do not vary so much, while the values of

(12) Schaftenaar, G.; Noordik, J. H. *J. Comput.-Aided Mol. Des.* **2000**, *14*, 123.

**Table 2.** Binding Energy of the Reactions  $5n\text{C} + (5n + 5)\text{M} + 10\text{H} \rightarrow \text{C}_{5n}\text{M}_{5n+5}\text{H}_{10}$  and  $6n\text{C} + (6n + 6)\text{M} + 12\text{H} \rightarrow \text{C}_{6n}\text{M}_{6n+6}\text{H}_{12}$  ( $n = 1, 2$ ) (BE, kcal/mol), Lowest Lying Vibrational Frequencies ( $V_{\min}$ ,  $\text{cm}^{-1}$ ), Lengths ( $\text{\AA}$ ) of the M–M Bonds in M Cycles ( $r_{\text{M-M}(1)}$ ), M–M Bonds Parallel to the Central Axis ( $r_{\text{M-M}(2)}$ ), M–C Bonds ( $r_{\text{M-C}}$ ), and M–H Bonds ( $r_{\text{M-H}}$ ), Total Wiberg Bond Indices of the Carbon Centers ( $\text{WBI}_{\text{C}}$ ) and Transition Metals ( $\text{WBI}_{\text{M}}$ ), Energies of the HOMOs (eV), and HOMO–LUMO Energy Gaps (eV) of the Barrel-like or Tubelike Complexes

	BE	$V_{\min}$	$r_{\text{M-M}(1)}$	$r_{\text{M-M}(2)}$	$r_{\text{M-C}}$	$r_{\text{M-H}}$	$\text{WBI}_{\text{C}}$	$\text{WBI}_{\text{M}}$	HOMO energy	energy gap
$\text{C}_5\text{Ni}_{10}\text{H}_{10}$	−1721	85	2.48	2.43	1.84	1.64	3.50	2.05	−6.69	2.18
$\text{C}_5\text{Pd}_{10}\text{H}_{10}$	−1739	58	2.77	2.70	2.04	1.79	3.36	1.87	−6.97	2.41
$\text{C}_5\text{Pt}_{10}\text{H}_{10}$	−1902	196i	2.79	2.73	2.05	1.82	2.52	2.26	−7.02	2.58
$\text{C}_6\text{Ni}_{12}\text{H}_{12}$	−2096	63	2.51	2.42	1.83	1.64	3.50	2.06	−6.70	2.10
$\text{C}_6\text{Pd}_{12}\text{H}_{12}$	−2120	44	2.80	2.69	2.03	1.80	3.38	1.90	−6.92	2.33
$\text{C}_6\text{Pt}_{12}\text{H}_{12}$	−2334	20	2.80	2.72	2.04	1.82	3.54	2.28	−7.07	2.45
$\text{C}_{10}\text{Ni}_{15}\text{H}_{10}^a$	−2587	72	2.50/2.54	2.50	1.83/1.91	1.64	3.52	2.06/2.08	−5.80	1.74
$\text{C}_{10}\text{Pd}_{10}\text{H}_{12}^a$	−2563	48	2.79/2.78	2.80	2.01/2.12	1.79	3.38	1.90/1.87	−5.92	1.78
$\text{C}_{12}\text{Ni}_{18}\text{H}_{12}^a$	−3158	56	2.54/2.61	2.47	1.81/1.91	1.64	3.60	2.07/2.07	−5.83	1.64
$\text{C}_{12}\text{Pd}_{18}\text{H}_{12}^a$	−3126	39	2.82/2.84	2.78	2.00/2.11	1.80	3.44	1.92/1.87	−5.94	1.66

<sup>a</sup> These species are located by 2D extensions of  $\text{CM}_4\text{H}_4$  ( $\text{M} = \text{Ni}, \text{Pd}$ ) units.

$\text{WBI}_{\text{M}}$  of the M atoms with octacoordination increase slightly. In addition, the tubelike molecules have higher HOMO energies and lower HOMO–LUMO energy gaps than the barrel-like molecules.

## Conclusions

In summary, we found for the first time that the structural units of  $\text{CM}_4\text{H}_4$  ( $\text{M} = \text{Ni}, \text{Pd}, \text{Pt}$ ) containing ptC could be extended naturally in one and two dimensions at the density functional theory level. Such extensions give us a series of piecelike, barrel-like (1D extensions), and nanotube-like (2D extensions) molecules, which contain more than one independent ptC or qptC. Calculations of the NBO and NICS behaviors revealed that it was the gradually enhanced aromaticity that acts as a dominant factor in maintaining the existence of several independent ptC atoms in a hydrometal complex. All these molecules are neutral species with regularly arranged intramolecular atoms, which may rebond to form further periodic extensions and then to form 1D or 2D crystals. Therefore, it is reasonable to imagine that it should be hopeful for synthetic chemists to prepare such substances in a macroscopic quantity in chemical laboratories. Because such molecules contain not only carbon atoms in a peculiar bonding geometry but transition metals such as Ni, Pd, and Pt, which possess high catalytic

activity, the experimental confirmation of these species will open and extend a new field in the bonding chemistry of carbon and may offer new high-efficient catalysts and materials with interesting characteristics.

**Acknowledgment.** This work was supported financially by the National Natural Science Foundation of China (Grant No. 30470408), Provincial Natural Science Foundation of Shanxi (Grant No. 2006011018), and Scientific Research Fund of Shanxi University.

**Supporting Information Available:** B3LYP-optimized geometries (in internal coordinates) and lowest vibrational frequencies of Ni-containing molecules with the LANL2DZ basis set for Ni atoms and the 6-311++g\*\* basis set for C and H atoms and those of Pd- and Pt-containing molecules with the CEP-31G or SDD basis set for Pd and Pt atoms and 6-311++g\*\* for C and H atoms, electron density analysis for the orbitals of  $\text{CNi}_4\text{H}_4$  involved in C–Ni bonding, and pictures of the HOMO, LUMO, and occupied  $\pi$  MOs concerning the  $2p_z$  orbital of the ptC centers of Pd- and Pt-containing molecules. This material is available free of charge via the Internet at <http://pubs.acs.org>.

OM070058N